CORIUM-RELATED IMPROVEMENTS IN THE EDF VERSION OF MAAP CODE IN THE FRAME OF SEVERE ACCIDENT STUDIES

E. Beuzet[1], N. Bakouta[1], M. Boissavit[1], F. Haurais[1,2], A. Le Belguet[1], V. Lombard[1], M. Torkhani[1]
[1]Electricité de France R&D
1 Avenue du Général de Gaulle, 92141 CLAMART, France
[2]Université Paris-Sud, Institut de Physique Nucléaire d'Orsay,
91406 ORSAY, France
emilie.beuzet@edf.fr, nikolai.bakouta@edf.fr, martin.boissavit@edf.fr, florian.haurais@edf.fr, alix.le-belguet@edf.fr, virginie.lombard@edf.fr, mohamed.torkhani@edf.fr

ABSTRACT

In some low probability situations, severe accidents in PWRs can lead to core degradation and relocation of molten material, called corium, from the core into the lower head. Heat exchange between the resulting corium and the vessel may lead to its failure. Ex-vessel phenomena such as High Pressure Melt Ejection (HPME) or Molten Corium Concrete Interaction (MCCI) can also occur in some situations and are key issues for safety analysis. In the frame of safety studies, all these mechanisms have a high priority not only to improve the EDF version of the MAAP code but also to maintain it at the state of the art of the international R&D. This specific version is also suitable for analysis of French PWRs.
In order to develop and validate the EDF models in MAAP, the common methodology applied is based on phenomenological studies and separate effect tests aiming at establishing physical and numerical models. Models and correlations are then implemented in the severe accident code and validated against more prototypical experiments. Reactor cases, also presented in this paper, aim at quantifying the contribution of these models, compared to the previous EDF version of MAAP, and giving recommendations for safety studies. Such improvements enable a better accuracy and a higher confidence in simulation tools for reactor safety studies. They are part of the EDF R&D MAGESTIC project.
As a focus, recent improvements of the MAAP code are presented in this paper. They deal with cladding degradation, corium stratification, MCCI, Fuel Coolant Interaction (FCI) and HPME. These new models take into account cladding nitriding, a better assessment of the corium stratification and focusing effect, the heat generated during FCI and the ejected liquid corium fraction during HPME.
The results presented in this paper show that the EDF models implemented in the MAAP code:

- are well validated against separate effect tests,
- show improvements compared to some standard models and to separate effect and integral tests,
- are suitable for reactor safety case calculations.

Future plans are also detailed in terms of experiments and modeling needs.

KEYWORDS
MAAP, cladding degradation, corium stratification, FCI, MCCI, HPME

1. INTRODUCTION

A severe accident is an unlikely sequence in which the reactor core is highly degraded. It is generally due to a loss of coolant, which implies that the core decay heat can no longer be removed due to accumulation of failures (human and/or material), including safety devices. Combined with a loss of the containment integrity, the core meltdown can lead to radiotoxic releases into the environment: this constitutes the source term.

Several steps characterize a severe accident. Following a loss of cooling in the primary circuit due to loss of cooling, core uncovery occurs. Fuel is heated due to the residual power and it can result in core degradation. Cladding oxidation by steam amplifies heat release, produces hydrogen and increases Fission Products (FP) release. Chemical reactions between the various materials in the core region lead also to core degradation resulting in the formation of a molten pool called corium. This melt can relocate to the bottom of the vessel. In this situation, a thermo-mechanical load on the vessel walls is created due to the interaction with corium is produced and can lead to vessel rupture. A part of the core may remain intact, as it was in TMI2 accident, while created corium can flow out of the vessel, at high or low pressure, and accumulate in the reactor cavity. This is the so-called Molten Corium-Concrete Interaction (MCCI), which induces reactions between corium and concrete.

Based on the concept of defense in depth and although this kind of accident remains highly unlikely, the impact that radioactive release could have onto the environment underlines the importance to study severe accidents and mitigation measures.

The present paper deals with in-vessel and ex-vessel phenomena tackled in the frame of the EDF R&D project called MAGESTIC, from the initial core degradation, the way corium stratifies, corium ejection and fragmentation to MCCI.

2. IMPROVEMENT METHODOLOGY OF MAAP CODE

MAAP (Modular Accident Analysis Program) is a Severe Accident (SA) integral code used to simulate the response of LWRs to severe accident sequence. It has been developed by FAI (Fauske and Associates Inc.) for EPRI (Electric Power Research Institute) since the Three Mile Island accident [1]. MAAP is a recognized code that is used worldwide. MAAP models the major physical phenomena occurring during an overall accident sequence in a small computational time. Numerous phenomena are modeled in order to account for thermal-hydraulics and fission products.

EDF has its own development license and validation process to cope with specific French PWR characteristics and also to take into account the international R&D. These two points constitute a high priority objective of the MAGESTIC project. Models developed by EDF are regularly transferred to FAI and implemented in the current version of MAAP.

The models describing the underlying physics have to be validated to guarantee better accuracy and enhanced confidence in numerical simulation results. As described in Figure 1 [2], improvements of the MAAP code is directly obtained thanks to the study of separate-effect tests, allowing the characterization of every non independent phenomenon occurring in a SA. The validation is also achieved through semi-integral tests. Then, the use of such “industrial” models can be recommended in safety analyses for complete reactor cases.

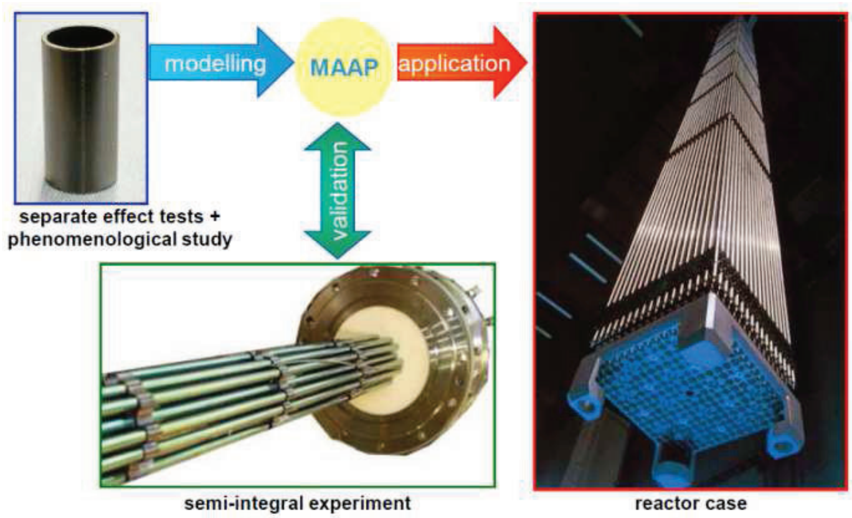

Figure 1. Methodology applied to improve the MAAP code, adapted from [2]

3. RECENT IMPROVEMENTS ON CLADDING DEGRADATION

3.1. Phenomenology of cladding oxidation

At high temperatures typical of SA sequences, the contact between Zr-based fuel claddings and vaporized water leads to a fast reaction between Zr and H_2O, producing ZrO_2 and H_2.

This exothermic reaction is detrimental for several reasons:
- It generates heat which enhances the temperature increase;
- It produces H_2, a gaseous compound which is potentially detonating under certain conditions;
- It progressively modifies the composition (from Zr to ZrO_2) and properties of fuel claddings.

Once a zirconia layer (ZrO_2) is formed at the cladding surface, this oxidation is mainly limited by the oxygen diffusion and depends on the state of this zirconia layer. Indeed, if it is intact and compact, the oxidation rate continuously decreases over time due to the progressive thickening of this protective layer. On the contrary, if it is cracked and porous, the oxidation rate remains constant over time [3].

In case of a vessel failure inducing air ingress into the reactor core, O_2 and N_2 react with Zr-based fuel claddings, through a self-sustained process involving three chemical reactions [4,5]: Zr reacts first with O_2 and, in case of O_2 starvation, with N_2. However, as soon as fresh oxygen is newly available, the Zr oxidation takes place again, together with the oxidation of the nitride (ZrN). As Zr, ZrN and ZrO_2 have different molar volumes, this self-sustained process strongly destabilizes the zirconia layer and enhances its degradation. Indeed, in air-steam mixtures, the zirconia layer becomes much more cracked and porous than under pure steam, and the corrosion rate is significantly accelerated as shown in recent innovative porosimetry studies [6].

3.2. Cladding oxidation modeling in MAAP and recent improvements

In the MAAP4 SA code, cladding oxidation by steam as well as by air relies on weight gain correlations based on separate-effect tests. Nitriding is not part of the official version of the code which concretely means that, in case of an oxidant starvation, nitrogen does not react with Zr although available in the gas. A nitriding model was thus implemented, also based on weight gain correlation. This correlation characterizes a mass gain per surface unit X (in $kg_{Zr}.m^{-2}$) as a function of temperature. Arrhenius-type laws are used to consider the temperature dependence of the reaction rate:

$$K_m(T) = A.e^{\frac{-E_a}{RT}}, \qquad (1)$$

with: A the pre-exponential factor (in $kg^n{}_{Zr}.m^{-2n}.s^{-1}$), E_a the activation energy (in $J.mol^{-1}$), R the universal gas constant and n corresponding to the order of the selected correlation.
This mass gain is expressed in terms of a thickness, which stands for the growth of the ZrN layer accounted for as Zr:

$$x^n = \frac{K_m(T).t}{\rho^n}, \qquad (2)$$

with ρ zirconium density in $kg.m^{-3}$ and rate constant K_m in $kg^n.m^{-2n}.s^{-1}$.

Original experimental data were used to define a new correlation as no correlation available in the literature reproduced all particular aspects of nitriding. This correlation is based on an experimental study dealing with the reaction between α-Zr(O) and nitrogen [7]. The obtained parameters for the KIT-EDF correlation [8] are presented in Table I.

Table I. Parameters for nitriding modeling with the KIT-EDF correlation

Temperature (K)	A	E_a	n
T <1173	7.23 10^6	2.98 10^4	1
1173 ≤ T < 1273	6.8 10^{-5}	3.44 10^1	1
1273 ≤ T < 1473	1.2 10^8	3.57 10^4	1
T ≥1455	3.8 10^{-8}	-1.62 10^4	1

Switch from oxidation to nitriding is done for a very low oxygen flow rate (O_2 flux < 10^{-8} $kg.s^{-1}$ and O_2 flux / N_2 flux < 10^{-2}), characterizing oxygen starvation conditions. Switch from nitriding to oxidation is automatically done in case of an available oxygen flow rate.

3.3. Example of validation: simulation of QUENCH-16

Nitriding modeling has thus been validated against semi-integral experiments, such as QUENCH-16 experiment [9] considered as a reference case for the study of cladding oxidation by air.
In a few words, the test section is composed of a 21-rod simulator bundle with various inlets for steam, air and water. 20 rods of this bundle are electrically heated by tungsten heaters, the central one being unheated.
The bundle and the facility have been modeled in MAAP as well as the different injection flow rates accounted for as boundary conditions. Figure 2 represents the thermal behavior of the QUENCH-16 bundle during the overall transient, in black for the experiment, in blue for calculated temperatures without the nitriding model (only oxidation model) and in red with the nitriding model (oxidation with nitriding) [8].

The three main steps composing the test transient are reproduced, namely:

- A steam pre-oxidation of the bundle to represent the core uncovery phase,

- An air oxidation, after an intermediate cooling, to study the impact of an air ingress on a corroded bundle,
- A bottom water reflood to put the bundle in a safe state and to study the impact of a reflood on a degraded bundle.

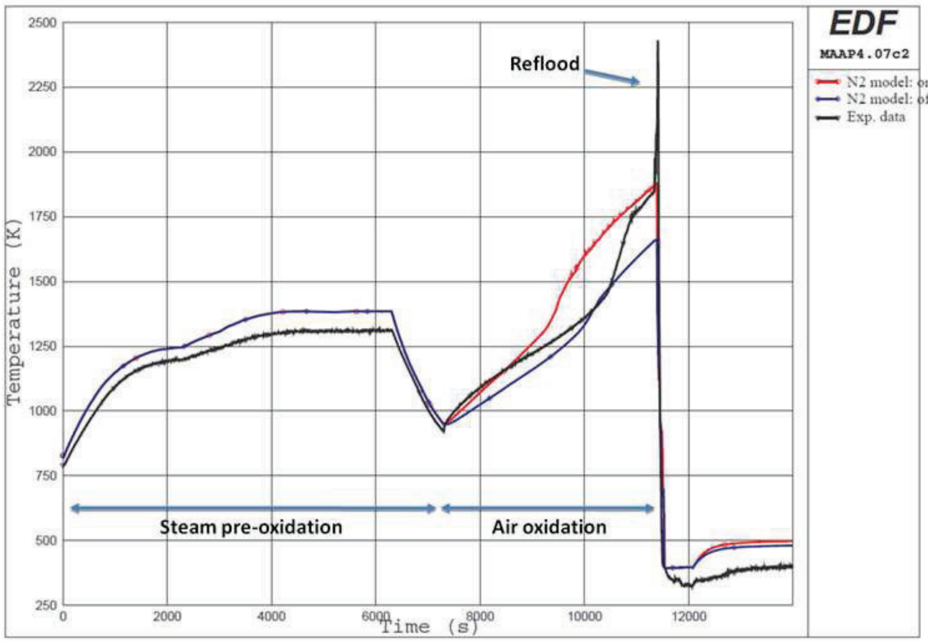

Figure 2. Claddings temperature at 850 mm during QUENCH-16 transient

A slight temperature over-estimation is visible on Figure 2 but the new version with nitriding model activated allows to reach the same value as the experiment at t=11330 s (time before quenching) whereas the previous version without using the nitriding model underestimates it by about 180 K. However the temperature escalation leading to this value occurs approximately 1000 s earlier. Nonetheless this was chosen as the best compromise, as it resulted in a hydrogen production by re-oxidation of nitrides in good agreement with the experiment, in comparison with the impact on the thermal behavior [8].

3.4. Synthesis

Regarding cladding oxidation, hydrogen production is a key parameter for safety in the analysis of severe accident scenarios, and this study is a step further in modeling it more accurately. Taking into account nitriding in MAAP has led to a better accuracy of hydrogen production. As the precise oxide layer structure is not described in MAAP, the oxidation of the cladding by steam penetrating the porous oxide layer during the reflood is not modeled. Further studies are thus necessary to improve the treatment of this phenomenon in MAAP by taking into account the exact composition of the degraded oxide layer, particularly the dissolved oxygen concentration, the evolution of the different oxide layers, their porosity and the crack formation, along the different stages of the scenario [6].

4. RECENT IMPROVEMENTS ON CORIUM STRATIFICATION

4.1. Short presentation of EDF's proprietary modeling

In MAAP 4, the corium pool is segregated into a set of horizontal layers in the Lower Head (LH). The mutual positioning of the layer is fixed as follows: oxide in the bottom, upper refractory crust, molten metal and debris particle bed on the top.

The possibility of a stratification inversion between oxide and metal phases under miscibility gap conditions has been demonstrated in numerous experimental programs (MASCA [10], CORDEB). In this case, the heavy metal layer containing metallic uranium could appear below the oxide layer leading to the thinning of the light metal layer and to an increase of the focusing effect.

According to the phenomenology deduced from those experiments, corium in-vessel models have been updated in several severe accident codes, especially in the version 5 of MAAP. Additionnally, the EDF proprietary version of MAAP has been adapted thanks to a combined CEA/EDF collaboration. The model's main features are presented below [11]:

- The pool is composed of the layers under a chemical equilibrium (heavy metal, oxide and light metal), the upper crust, a layer of out-of-equilibrium metal and the solid debris bed.
- The layers in equilibrium are surrounded by a refractory crust with a boundary condition $T_{liquidus}$ of the mix [12]. The composition of the transient layers tends to the final composition in equilibrium. This was calculated using Salay and Fichot method [13].
- The out-of-equilibrium metal layer stands in direct contact with the vessel with a side limit condition of T_{steel_fusion}. The highest heat transfer to the pressure vessel (and the point of the most likely failure), the so-called "focusing effect", is expected to take place through this layer. Moreover, it is supposed that the metal of this layer could go down through the crust leading to stratification inversion, see Figure 3 below.

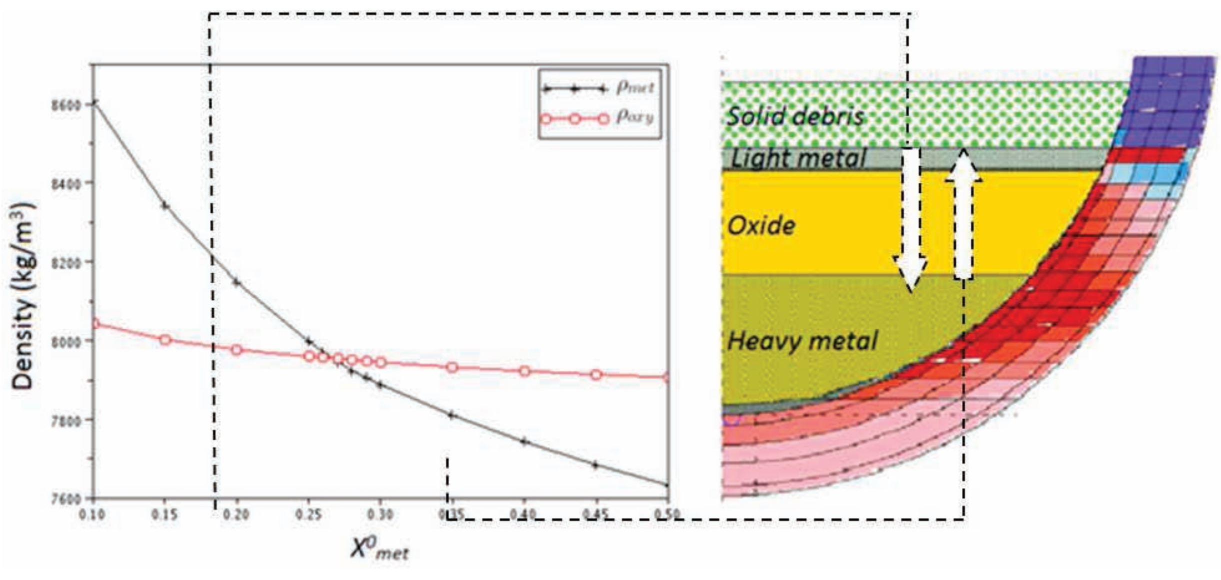

Figure 3 Transient metal stratification in the LH depending on the steel fraction in pool X^0_{met}

Contrary to the MAAP's standard modeling, the kinetic of layers inversion [14] is taken into account when the transient layers tend to an equilibrium configuration. This configuration is given by a simplified thermochemical model [13] providing compositions of the oxide and metal phases. The decay heat is divided pro rata between the layers according to the concentration of uranium.
This modeling has been integrated in both MAAP 4 and MAAP 5 EDF-proprietary versions.

4.2. Reactor case example

Continuous validation of this "prospective model"of the MAAP EDF-proprietary version is still under progress. For now, it cannot be used directly for safety analysis, but can give an overall idea of the corium behaviour for a reactor case. For example, in the case presented in Figure 4 with the initial state "A", we can see a maximum heat flux to the vessel corresponding to the initial formation of a steel layer (B). The vessel heating needs some time to reach equilibrium, so the opposite external flux appears later (C). At this stage, the internal heat flux was already decreased due to the layer thickening and finally could be balanced by external cooling (D). These results correspond of course to a particular scenario and need further validation.

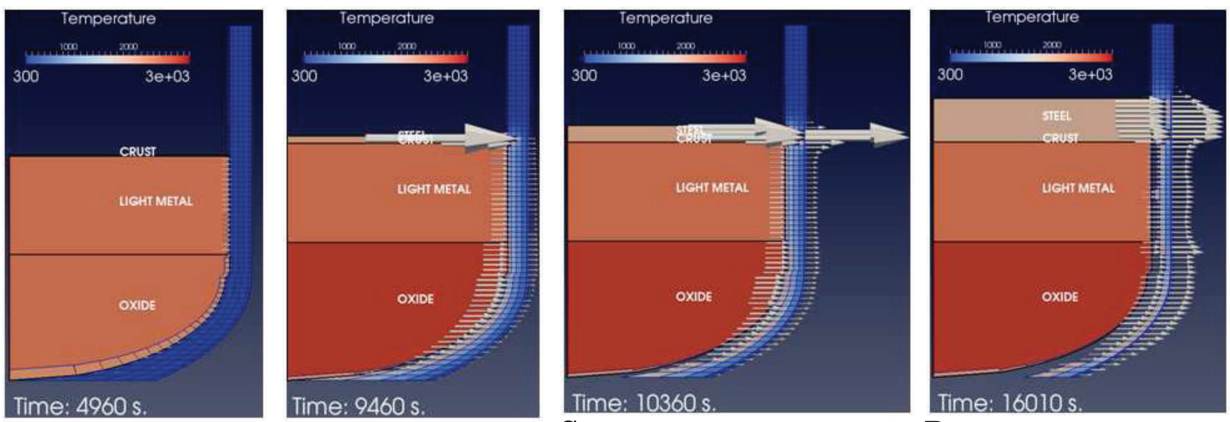

A B C D

Figure 4. Key moments of a reactor case simulation

4.3. Synthesis

On corium stratification modeling, huge developments were made at EDF to take the different layers formation, their composition and above all the possibility of a stratification inversion into account. Further validations are needed, both on benchmarks and reactor cases, on topics such as vessel ablation and debris coolability. This work is promising and is a key model for in or ex-vessel corium issues. This study has also underlined the importance of T_{liq} and T_{sol} prediction as it governs the overall accident progression, motivating further works on thermochemistry.

5. ASSESSMENT OF MOLTEN JET FRAGMENTATION MODELING IN MAAP

Molten corium resulting from core degradation can interact with the remaining water during its relocation in the lower head or in the reactor pit. As corium jet penetrates water, it undergoes instabilities due to counter-current vapor flow resulting from water vaporization. This leads to jet break-up and droplet formation, whose description is required to evaluate FCI consequences. For more details, one may refer to [15].

5.1. Jet fragmentation modeling in MAAP

Jet fragmentation modeling in MAAP is based on entrainment similarity assumption using Ricou-Spalding [16] correlation to evaluate the jet entrainment mass rate, $\dot{m}_{ent}$. This is expressed as:

$$\dot{m}_{ent} = E_0 A_{Sj} \left(\frac{\rho_w}{\rho_j} \right)^{1/2} \rho_j U_j \tag{3}$$

with E_0 the entrainment coefficient, A_{Sj} the jet surface area, U_j the jet velocity as it reaches water surface, ρ_j (resp. ρ_w) the jet (resp. water) density.

Besides, Saïto and Meignen correlations can be used to evaluate E_0, depending on a user-defined parameter, I_{E0}:

- if $I_{E0} = 0$: E_0 is a constant defined by a user-defined parameter, $E_{0,Const}$,
- if $I_{E0} = 1$: E_0 is evaluated from Saïto correlation [17]:

$$E_0 = \frac{(gD_{j,0})^{1/2}}{2F_{Saïto} U_j} \tag{4}$$

where g is the gravitational acceleration, $D_{j,0}$ the initial jet diameter and $F_{Saïto}$ a user-defined constant.

- if $I_{E0} = 2$: E_0 is determined using Meignen correlation [18] given by:

$$E_0 = \frac{0.1}{U_j} \left(\frac{\rho_j}{\rho_w} \right)^{1/2} \tag{5}$$

Other input parameters related to the average void fraction, α_V, to the size of particles resulting from jet erosion, F_{Dp}, and to the final particle temperature, I_{Dp}, may impact jet fragmentation mechanism and heat transfer, affecting as well pressure and temperature levels. These parameters, whose effect is studied through a sensitivity study (cf. paragraph 5.2), are listed in Table II.

Heat transfer from corium to the surroundings during melt relocation turns out to be overestimated in MAAP bench mode. This is caused by the release of all corium energy to liquid water and vapor. Therefore, the calculation of heat transfer from corium melt has been corrected by taking into account final particle temperature. This is the only modification that has been done in the jet fragmentation modeling so far.

Table II. Parameters affecting jet fragmentation in MAAP

Studied parameters		**Default**	**Min.**	**Max.**	**Impact**
Entrainment coefficient (if $I_{E0} = 0$)	$E_{0,Const}$	0.045	0.025	0.06	+
Correlation used to evaluate E_0	I_{E0}	0	0	2	+
Saïto correlation coefficient, $F_{Saïto}$	$F_{Saïto}$	2.1	2	2.2	+
Average void fraction in the interaction zone	α_V	0.25	0.1	0.3	-
Size of particles resulting from jet erosion	F_{Dp}	0.63	0.5	0.75	++
Final particle temperature	I_{Dp}	1	0	1	++
Evaluation of heat transfer from corium		With or without modification			+++

5.2. Simulation of FARO experiments: focus on L-28 test

Simulation of FARO experiments have been carried out to assess the relevance of jet fragmentation modeling in MAAP (version 4.08a). FARO is a large-scale experimental program conducted to investigate MFCI and quenching behavior under both in- and ex-vessel severe accident conditions [19]. In this test, 175 kg of prototypic corium at 3052 K are poured by gravity in a saturated water pool, resulting in debris formation and an increase of pressure and temperature levels.

MAAP predicts a coherent rise in pressure (Figure 5) and temperature, particularly when:

- taking into account the modification of heat transfer calculation,
- using Meignen correlation ($E_0 = 0.076$) which gives the best estimation of the jet break-up length,
- using F_{Dp} default value ($F_{Dp} = 0.63$).
- evaluating a consistent final particle temperature ($I_{Dp} = 1$).

This dataset allows to re-calculate other FARO experiments, with good results.

As shown in Figure 5, corium jet fragmentation is complete beyond a threshold value of the entrainment coefficient E_0 ($E_{0,\ threshold} \approx 0.034$ for L-28 test) and thus, E_0 has no more impact on jet fragmentation. The computed final particle size ($D_{p,\ MAAP} = 4.43$ mm) is in agreement with the mean diameter of collected debris in L-28 test ($D_{p,\ L\text{-}28} = 3.64$ mm). The average void fraction has no overall effect on pressure or on temperature levels, which is quite unexpected and counter-intuitive. Moreover, it remains constant during melt injection in MAAP. The void fraction is obviously not correctly taken into account in jet fragmentation modeling in MAAP. More details can be found in [15].

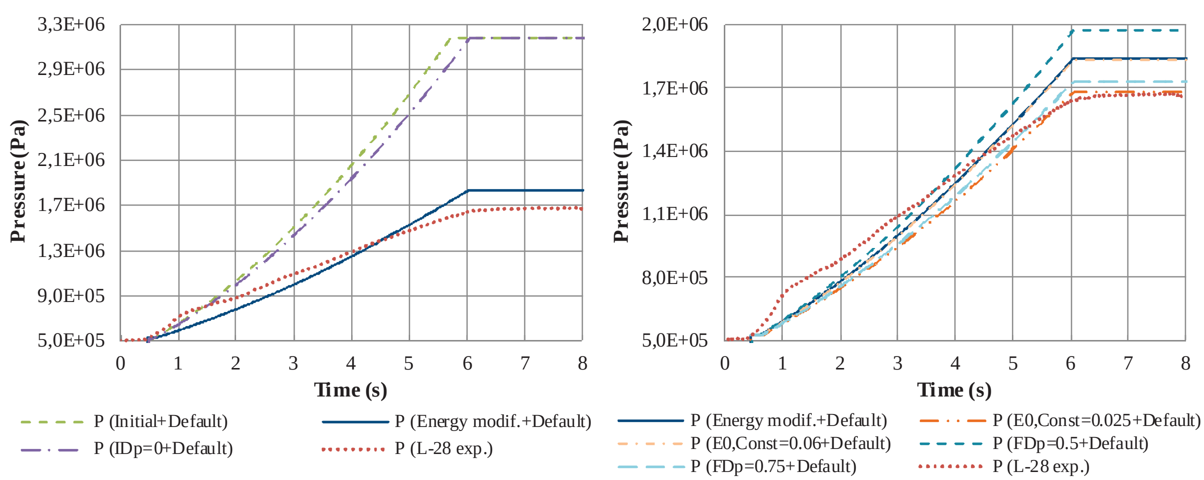

Figure 5. Pressure: comparison of L-28 test results to MAAP simulations

5.3. Synthesis

The simulation of FARO experiment, supplemented by a preliminary model analysis of MAAP subroutines, showed that MAAP predicts a coherent rise in pressure and temperature with a unique dataset. Nevertheless, it suggested improvements of jet fragmentation modeling such as:

- implementing new correlations describing jet fragmentation,

- taking into account void fraction in jet erosion and heat transfer as well as its evolution during melt relocation,
- improving the evaluation of debris size or heat transfer between melt and the surrounding environment.

Enhancements identified as the most relevant should be integrated in the next released version of MAAP and validated against experimental data.

6. MAIN RECOMMENDATIONS ON HPME MODELING

A previous sensitivity analysis of various severe accidental scenarios of a 900 MWe PWR showed that the fraction of dispersed corium from Kim's correlation may be limited by the pool liquid fraction calculated in MAAP during its discharge into the reactor pit. To investigate whether this limitation is justified or not, the more recent correlation established by IRSN with multidimensional multiphase flow code MC3D to calculate the out of cavity dispersion [20] has been introduced in MAAP 4.07 code. The impact analysis of suggested improvements was performed during a benchmark of an IET-10 test [21].

6.1. Overall phenomenology

During a PWR severe accident, if a vessel failure occurs, the corium pool in the vessel lower head is ejected into the reactor pit together with steam, possibly hydrogen coming from the primary circuit and remaining liquid water. Depending on the vessel break size and primary circuit pressure at vessel failure, the ejection induces a more or less fine fragmentation of corium and dispersion of fragments out of the reactor pit, see Figure 6. This corium drop dispersion leads to very efficient heat exchanges between corium itself and the containment atmosphere. The main part of the corium does not remain in suspension in the gas stream, but is spread in the reactor pit - even up on the vertical walls under a velocity effect. The gas is ejected from the reactor vessel at its failure, then goes to the containment compartments connected to the reactor pit, well carrying with it the corium.

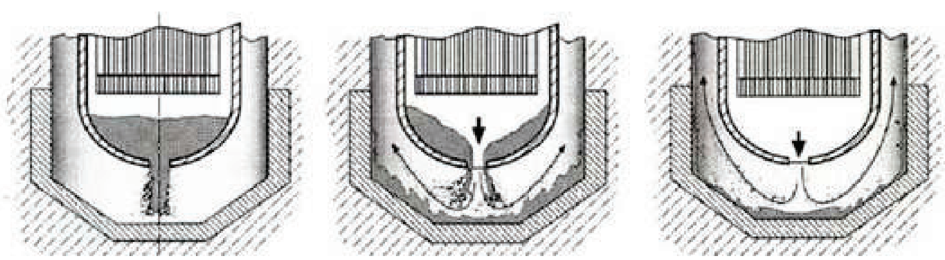

Figure 6. Illustration of melt corium entrainment out of the bottom pit [23]

6.2. Corium dispersal modeling

The corium dispersal following high pressure vessel failure is a complex phenomenon that cannot be precisely modeled in integral MAAP code as it could be with a CFD code for example. In the MAAP4.07 version, its modeling is simplified using Kim's correlation.

$F_{dispersed}$, the fraction of the corium dispersed out of cavity after high pressure vessel failure, can be evaluated as follows [22]:

$$F_{dispersed} = 0{,}4 * \left(1 + \tanh\left(3{,}79 \log \frac{t^*}{15}\right)\right) \tag{6}$$

with the non-dimensional parameter $\mathbf{t}^*$ equal to :

$$t^* = \frac{(\rho_{water}/\rho_f)^{0,5}}{L_p(1-\gamma)} \cdot \frac{1}{\rho_g A_v} \left(\frac{P_v^0 V_v^0}{RT_v^0}\right)\left(1 + \frac{V_g^{\min}}{V_g^0}\right)\left(1 - \left(\frac{V_g^{\min}}{V_g^0}\right)^{\frac{1-\gamma}{(1+\gamma)}}\right) \tag{7}$$

with ρ_f the corium density (kg.m^{-3}), L_p the debris path length (m), ρ_g the gas density (kg.m^{-3}), A_v the area of vessel bottom failure (m^2), P_v^0 the vessel pressure at HPME (Pa), V_v^0 the corium ejection velocity at HPME (m.s^{-1}), T_v^0 the vessel gas temperature at HPME (m.s^{-1}), $V_g^{\min}$ the minimum gas velocity for entrainment (m.s^{-1}) and V_g^0 the mean out-of-cavity gas velocity (m.s^{-1}).

With the aim of maintaining the MAAP code at the state of art, EDF has examined a more recent corium dispersion correlation. IRSN has established a new debris dispersal correlation after HPME. This correlation was particularly validated on the DISCO P'4 facility and is written as follows [20]:

$$F_{dispersed} = 0{,}45 * \left(1 + \tanh\left(5 * \log \frac{\sqrt{K*}}{170}\right)\right) \tag{8}$$

The $\sqrt{K*}$ dimensionless parameter is defined is given by:

$$\sqrt{K*} = 0{,}56 * \left(\frac{A_v}{A_a}\right)^{1/4} \frac{P_v^0}{\sqrt{T_v^0}} \sqrt{\frac{\gamma M_c}{R}} \left[\rho_f g \sigma\right]^{-1/4} \frac{1}{\sqrt{\rho_0}}, \tag{9}$$

with: A_a the annular compartment area (m^2), A_v the area of vessel bottom failure (m^2), M_c the molar mass (kg.mol^{-1}), σ the surface tension (N. m^{-1}), ρ_0 the reference density = 1 kg.m^{-3}.

6.3. Impact of the new correlation

Once the new correlation was implemented in MAAP4.07 code, its dispersion prediction was analyzed and compared to the Integral Effect Test IET-10.

The IET experiments were part of a NRC experimental program and represented major integral and separate effect tests to resolve the long-standing severe accident issue of HPME and its consequences. In all IET tests, a chemically reactive melt of thermite or corium at high temperature is ejected from a melt generator by high-pressure steam into a scale model of reactor cavity similar to French PWR pit. Debris was entrained by the steam blowdown into a large test vessel simulating a reactor containment building. All details regarding the IET-10 test are given in [21].

Moreover, in order to check the legitimacy of the dispersed corium's limitation of its liquid fraction, the impact analysis above was extended to investigate modeling of IET-10 test on corium liquid fraction. As EDF has access to MAAP4.07 source code, some tests related to parameters influencing corium dispersion have been made and their impact is analyzed (dispersal limitation by corium liquid fraction, implementation of new correlation).

Thereby Table III presents MAAP results obtained with Kim's/New correlation with/without liquid fraction limitation of the corium pool compared to experimental findings of the IET-10 test.

Table III. IET-10 test: impact analysis of dispersion correlation and liquid fraction limitation in MAAP4.07 code

Dispersed fraction out of cavity	Experimental value	Kim's correlation	New correlation
with liquid fraction limitation	*73%*	60%	60%
without liquid fraction limitation	*73%*	79%	89%

In this HPME benchmark, the corium liquid fraction limitation of MAAP gives the same dispersed fraction between both correlations. Indeed, in MAAP 4.07 code, it is originally considered that the effective dispersed fraction is strictly equal to the liquid part of the corium discharged at vessel failure. The experimental value could be then underestimated. Conversely, when the dispersed fraction is no longer limited, then the effective corium dispersed fraction is equal to the one calculated by Kim's correlation and by the new correlation. In that case, both correlations overestimate the experimental value but Kim's seems to be more suitable. The dispersed fraction coming from the new correlation appears excessive regarding HPME consequences. Further benchmarks have to be done to consolidate these outcomes.

6.4. Synthesis

This HPME benchmark study is the first step of a comparative analysis of correlations evaluating the fraction of dispersed corium following HPME. In-depth work in MAAP code is intended. The liquid fraction of discharged pool appears to be a limiting factor for dispersion. Therefore the next step is to establish an improved model for the corium fragmentation before and during HPME and its integration with other MAAP models (e.g. corium stratification). Another issue is to continue the comparative analysis of the considered correlations for containment pressure estimation related to hydrogen production.

7. ANALYSIS OF MCCI TREATMENT IN MAAP5

This part presents the modeling of MCCI in the FAI/EPRI version of MAAP5 with its improvements in the modeling of heat transfer from the molten corium to the water above it. MCCI phenomena refer to the interactions between the corium in the reactor cavity and the concrete as well as all the phenomena that occur consequently such as chemical reactions inside the molten corium pool, molten corium – water heat transfer, etc.

7.1. Modeling of MCCI in MAAP5

The modeling of MCCI in MAAP takes into account the following main phenomena of MCCI:

- Heat transfer between the concrete walls of the cavity and the corium. This model includes the calculation of the crust and the interface temperatures;
- Concrete ablation;
- Heat transfer between the corium and the atmosphere above (liquid water, steam, air);
- Chemistry of the corium pool.

The heat transfers between the corium and the water above the upper crust have been improved by taking into account two important mechanisms: 1) the corium eruption driven by the off-gas from MCCI through the upper crust and 2) the water ingression inside the cracks of the crust.

The corium eruption is modeled by the Ricou-Spalding model [16] which is further detailed in paragraph 5.1. When the off-gas velocity is high enough, a molten corium part is entrained through the crust as small particles. These particles are in direct contact with the water above and are added to the particle bed above the upper crust. Steam is produced by this transformation and the entrained corium can solidify [24]. This implies a quicker pressurization of the containment and a higher cooling of the corium pool, which is supposed to consequently reduce the wall ablation.

The second mechanism is water ingression inside the cracks of the upper crust. It is modeled by the Epstein-Lister model [25], which has been validated by the SSWICS tests at the Argonne National Laboratory (ANL). The cooling main effect of this water ingression is the decrease of the molten corium temperature in the cavity.

7.2. Effect of recent MAAP5 improvements on a total loss of steam generator feedwater supply on a reactor case

The methodology which was applied for the present study aims at studying the effects of both Epstein-Lister model and Ricou-Spalding correlations [16] on reactor applications.

Table IV presents the results obtained for a total loss of steam generator feedwater supply on a French reactor using MAAP5, both without and with Epstein-Lister model and Ricou-Spalding correlations, respectively named as MAAP5_without and MAAP5_with.

Table IV. Results of different MAAP5 calculations without and with Epstein-Lister model and Ricou-Spalding correlations, respectively MAAP5_without and MAAP5_with

	MAAP5_without	**MAAP5_with**
Time of core uncovery (s)	3577.22	3577.22
Time of vessel failure -VF- (s)	26738.67	26738.67
Residual Power at VF (MW)	22.5	22.5
Ablated concrete volume (m^3)	10^{-4}	27.50
Time of containment failure (s)	191731.13	211184.88

These calculations show the impact of the two correlations on MCCI treatment, which has an effect only on the ex-vessel part of the calculation. These correlations impact the corium heat balance. A lower steam flow rate is calculated when these two correlations are taken into account, as seen on Figure 7. The pressurization is thus lower leading to the maintaining of the containment integrity but with a higher ablated concrete volume (due to heat removal in the concrete).

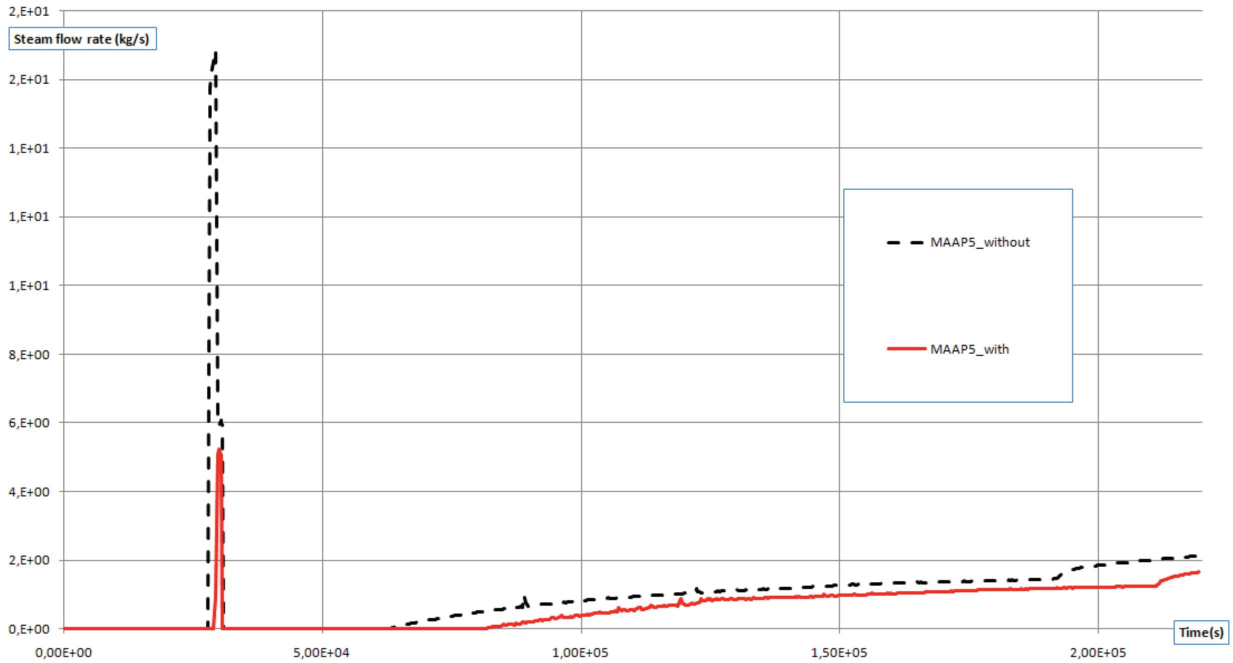

Figure 7. Steam flow rate calculated without and with Epstein-Lister model and Ricou-Spalding correlations, respectively MAAP5_without (in black dashed) and MAAP5_with (in full line red)

These calculations allow EDF to know the macroscopic effects of the recent improvements and how to adapt the user parameters to the French reactors. The difficulty of interpreting precisely the impacts of the modeling in integral calculations is to separate the positive and adverse effects on macroscopic variables, such as the delay to reach containment failure pressure and the volume of ablated concrete due to MCCI.

7.3. Synthesis

Based on recent MAAP 5 improvements, the EDF study has stressed the important impact of the FAI / EPRI new modeling on reactor applications. To better understand this impact and to rule on an industrial use of this modeling, benchmark comparison is needed on CCI tests, for instance between MAAP 5 and TOLBIAC-ICB which constitutes the reference code for MCCI studies at EDF. These comparisons between TOLBIAC-ICB, MAAP5 and experimental data will give EDF the opportunity to adapt its version of MAAP for MCCI calculations and have more precise results regarding containment pressurization.

8. CONCLUSIONS AND FUTURE PLANS

The present paper gives an overview of the large range of phenomena covered in the current version of MAAP and their representativity against benchmarks and reactor cases. It details also recent work done on corium-related improvements in the EDF version of MAAP. What is important to keep in mind is the systematic methodology to study each phenomenon at different scales and progressively incorporate them in the model. The defense-in-depth principle is continuously applied in French NPP safety. For instance, the international R&D work is being updated in the EDF version of MAAP severe accident code. Main improvements are regularly transferred to FAI and implemented in the current version of MAAP.

Improvements presented in this paper led to future plans, directly linked to this defense-in-depth principle. For instance, as the precise oxide layer structure is not described in MAAP, further work is thus necessary to describe the structure of the degraded oxide layer and its porosity. Further studies are also planned to improve modeling of the corium fragmentation before and during HPME and its correct interaction with other MAAP models (such as corium stratification). New correlations describing jet fragmentation and void fraction in jet erosion and heat transfer will make significant improvements to the MAAP code. This will impact on corium stratification (in-vessel) and also MCCI (ex-vessel) modeling. Validation is also needed on corium stratification in the lower head for topics such as vessel wall ablation and debris coolability. Benchmark comparison is currently underway on CCI tests, between MAAP 5 and TOLBIAC-ICB, the reference code for MCCI studies.

REFERENCES

1. F. Rahn, "Technical Foundation of Reactor Safety - Knowledge Base for Resolving Severe Accident Issues", *Technical Report 1020497*, EPRI, (2010).
2. M. Steinbrück et al.: 'Comparison of oxidation kinetics of advanced cladding alloys in steam at temperatures 600-1200°C', *Proceedings of the 14th QUENCH workshop,* ISBN 978-3-923704-67-5, (2008).
3. P. Sarrazin, A. Galerie and J. Fouletier, "Les mécanismes de la corrosion sèche - une approche cinétique", *EDP Sciences*, ISBN 2-86883-472-8, (2000).
4. M. Steinbrück et al., "Oxidation of advanced zirconium cladding alloys in steam at temperatures in the range of 600-1200°C", *Oxid Met*, **76**, pp. 215–232, (2011).
5. M. Steinbrück and M. Böttcher, "Air oxidation of Zircaloy-4, M5 and ZIRLO cladding alloys at high temperatures", *Journal of Nuclear Materials*, **414**, pp. 276–285, (2011).
6. F. Haurais, "Degradation mechanism of Zr-based fuel claddings in steam and air-steam atmospheres at high temperatures", presented at the 20th IQW, ISBN 978-3-923704-88-0, (2014).
7. M. Jung: "Untersuchungen zur Oxidationskinetik von Zircaloy-2 und Untersuchungen zur Reaktion von α–Zr(O) mit Stickstoff. Praxissemesterbericht (Interner Bericht, NUKLEAR 3425)", Hochschule Mannheim, Institut für Materialforschung (IMF I), (2011).
8. E. Beuzet, C. Baumgarten and M. Steinbrück, "Modelling of cladding oxidation by air under severe accident conditions with the MAAP 4 code", *Proceedings of TOPFUEL / WRFPM 2014*, 14-17 September 2014, Sendai, Japan.
9. J. Stuckert, M. Große, Z. Hózer and M. Steinbrück, "Results of the QUENCH-16 Bundle Experiment on Air Ingress", *Technical report KIT-SR-7671*, http://digbib.ubka.uni-karlsruhe.de/volltexte/1000034168, (2013).
10. M. Barrachin, F.Defoort, "Thermophysical properties on In-Vessel Corium: MASCA Programme Related Results", *Proceedings of MASCA seminar,* Aix-en-Provence, (2004).
11. L. Saas, R. Le Tellier, A simplified geometrical model for transient corium propagation simulation in core for an LWR with heavy reflector, accepted for publication in Proc. of International Congress on Advances in Nuclear Power Plants ICAPP'2015, Nice (France), May 03-06, 2015.
12. J.M.Seiler, A. Fouquet, K. Froment, and F. Defoort, "Theoretical analysis for corium pool with miscibility gap", *Nuclear Technology,* **141**, (2003).
13. M. Salay and F. Fichot, "Modelling of metal-oxide corium stratification in the lower plenum of a reactor vesse"l, *Proceedings. of Int. Topical Meeting on Nuclear Thermal-Hydraulics (NURETH-11),* Avignon, (2005).
14. G.Ratel, F.Deffort, K.Froment, B.Tourniaire and J.M.Seiler, "Considerations on mass transfer kinetics for layer inversion and layer oxidation: from MASCA program to the reactor situation", *Proceedings of MASCA-2 Seminar*, Cadarache, France, (2007).

15. A. Le Belguet, E. Beuzet, “Simulation of FARO L-28 and L-31 tests to assess molten jet fragmentation modeling in MAAP”, *Proceedings of the 16th International Topical Meeting on Nuclear Reactor Thermal-Hydraulics, NURETH-16*, August 30–September 4, 2015, Chicago, U.S. (2015). *To be published*.
16. F.P. Ricou and D.B. Spalding, “Measurements of entrainment by axi-symmetric turbulent jets”, *Journal of Fluid Mechanics*, **11**, pp. 21-32 (1961).
17. M. Saïto, K. Sato, K., S. Imahori, “Experimental study on penetration behaviors of water jet into freon-11 and liquid nitrogen”, *ANS Proceedings National Heat Transfer Conference*, Houston, U.S., **3**, pp. 173-183 (1988).
18. R. Meignen, “Modélisation de la fragmentation d’un jet liquide à très haute température dans un liquide froid volatile”, *PhD Thesis, INPG*, France (1995).
19. D. Magallon, I. Huhtiniemi, “Corium melt quenching tests at low pressure and subcooled water in FARO”, *Nuclear Engineering and Design*, **204**, pp. 369–376 (2001).
20. R. Meignen, T. Janin, “On the analysis and evaluation of direct containment heating with the multidimensional multiphase flow code MC3D”, *Science and Technology of Nuclear Installations*, **2010** (Article ID 289792), 13 pages (2010).
21. T. K. Blanchat, M. D. Allen, “Experiments to investigate DCH phenomena with large-scale models of the Zion and Surry nuclear power plants”, *Nuclear Engineering and Design*, **164**, pp. 147-174 (1996).
22. S. B. Kim, M. K. Chung, M. H. Kim, H. Y. Lee, “A parametric study of geometric effect on the debris dispersal from a reactor cavity during high pressure melt ejection”, *International Communications in Heat and Mass Transfer*, **22**, pp. 25-34 (1995).
23. B.R. Sehgal, P. Piluso et al., “Sarnet lecture notes on nuclear reactor severe accident phenomenology”, *CEA-R-6194*, **CEA Report**, (2008).
24. D. Jacquemain. *Les accidents de fusion du cœur des réacteurs nucléaires de puissance – Etat des connaissances*. Edp sciences. France (2013).
25. M. Epstein, *Review of Water Ingression Models*, ACEX-TR-C31, (2000).